Mode shape prediction model from ODS for beam structures

Bor-Tsuen Wang and Ying-Hui Wu

Department of Mechanical Engineering
National Pingtung University of Science and Technology

National Science Council Contract NO: NSC90-2212-E-020-004.

ABSTRACT

This paper presents the modal analysis for beam structures in harmonic operating conditions. The mode shape prediction model is developed with the use of operational deflection shape (ODS) of the beam. The modal and harmonic response analysis is first introduced. By the adoption of polynomial fitting technique to represent mode shape functions, the optimization problem to determine structural mode shapes from ODS can then be formulated and solved. Both the numerical simulation and experimental verification are performed to demonstrate the effectiveness of the prediction model. Results show that the structural mode shapes can be well predicted from ODS for either on- or off-resonance excitation case. This work thus enhances the modal parameter excitation technique for structure under harmonic operating conditions.

Keyword: modal analysis, operational deflection shape, mode shape, harmonic operating conditions

NOMENCLATURE

A_b	beam cross-sectional area
$a_{r,q}$	coefficient of polynomial fitting function
C_b	beam damping coefficient
E_b	beam Young's Modulus
F_j	amplitude of the j-th harmonic force
$F(x,t)$	excitation force function
$\{F(\omega)\}$	force vector
$H_{ij}(\omega)$	frequency response function between the i-th displacement and the j-th force
$[H(\omega)]$	frequency response function martix
I_b	beam cross-sectional area moment of inertia
L_b	beam length
MAC	modal assurance criterion
m	number of measurement point of ODS and also the number of mode shape components
N	order of the polynomial function
n	number of modes to be determined
p	number of interpolation points for polynomial fit
S_r	sum of the absolute value of mode shape components for r-th mode shape
S_{dr}	sum of the absolute value of derivative of r-th mode shape component
$w(x,t)$	beam lateral displacement
$X_i(\omega_e)$	i-th component of operational deflection shape for harmonic excitation
$\lvert X_i(\omega_e)\rvert$	absolute value of operational deflection shape for harmonic excitation
$\{X(\omega)\}$	displacement response vector
$\{X(\omega_e)\}$	operational deflection shape for harmonic excitation
$\{\hat{X}(\omega_e)\}$	experimental operational deflection shape for harmonic excitation
$y_{r,s}$	design variable of s-th component of the r-th mode shape
ξ_r	r-th viscous damping ratio
ρ_b	beam density
Φ	objective function
$\phi_{r,j}$	j-th component of the r-th normalized modal vector
$\phi_r(x)$	r-th mode shape function
$\{\phi\}_r$	r-th normalized modal vector
ω_r	r-th undamped natural frequency
ω_e	excitation frequency

1. Introduction

In performing conventional experimental modal analysis (EMA) or testing, structures are generally required to be in static. With the use of actuators, such as shakers or impact hammers, to excite structure and the use of sensors, such as accelerometers, to measure structure response, the frequency response function (FRF) can then be measured. At least a row or a column of FRF matrix should be obtained so that the general curve-fitting process can be applied to extract structure modal parameters [1]. If the test structure is in its operating condition, such as a rotor system in rotating condition, the conventional EMA technique can not be applied directly.

For the restriction of conventional modal testing, the structural modal identification in operational condition arises many interests. James *et al.* [2] proposed the natural excitation technique (NexT) to extract modal parameters from operating structures. Hermans and Auweraer [3] developed the modal identification method by using output-only response and discussed its use for real structures, such as bridges, aircrafts and vehicles. Hermans and Hermans [4] also introduced structural model identification during normal operating conditions.

The ODS is not only useful for machinery diagnosis [5] or damage detection [6] but also applicable to identify excitation force [7]. Wang [8] had a first attempt to extract mode shapes from ODS for MDOF systems. Hu [9] further modified the prediction model by adding realistic constraints and had experimentally validated the modal data for MDOF systems. This paper will adopt the basic idea from Wang [8] and Hu [9] to develope the mode shape prediction model from ODS for beam structures.

This work assumes the beam structure subjected to a known harmonic force excitation. The beam will also appears harmonic response. The ODS of the beam can then be measured and as the input data to the prediction model. The developed mode shape prediction model can identify the derived structural mode shapes. This work thus enhances the modal parameter extraction technique for structure under harmonic operating condition and can be extended to operational rotor system for extracting system mode shapes.

2. Theoretical Analysis

2.1 Modal analysis

Consider a beam neglecting shear deformation and rotary inertia. The equation of motion for lateral vibration can be expressed as follows:

$$E_b I_b \frac{\partial^4 w(x,t)}{\partial x^4} + C_b \frac{\partial w(x,t)}{\partial t} + \rho_b A_b \frac{\partial^2 w(x,t)}{\partial t^2} = F(x,t) \quad (1)$$

For the cantilever beam as shown in Fig. 1 fixed end at $x = 0$, the boundary condition can be shown:

$$w(x=0,t)=0 \; , \quad \left.\frac{\partial w(x,t)}{\partial x}\right|_{x=0} = 0$$
$$\left. E_b I_b \frac{\partial^2 w(x,t)}{\partial x^2}\right|_{x=L_b} = 0 \; , \quad \left.\frac{\partial}{\partial x}\left(E_b I_b \frac{\partial^2 w(x,t)}{\partial x^2}\right)\right|_{x=L_b} = 0 \quad (2)$$

Natural frequencies of the cantilever beam can be obtained as follows [10]:

$$\omega_r = (\alpha_r L_b)^2 \sqrt{\frac{E_b I_b}{\rho_b A_b L_b^4}} = (\alpha_r)^2 \sqrt{\frac{E_b I_b}{\rho_b A_b}} \quad (3)$$

where

$\alpha_1 L_b = 1.87510407$

$\alpha_2 L_b = 4.69409113$

$\alpha_3 L_b = 7.85475744$

$\alpha_4 L_b = 10.11554073$

$\alpha_5 L_b = 14.13716839$

For $r > 5$

$$\alpha_r L_b \approx \frac{\pi(2r-1)}{2}$$

The normalized mode shapes can be expressed:

$$\phi_r(x) = \frac{1}{\sqrt{\rho_b A_b L_b}}[\cosh \alpha_r x - \cos \alpha_r x - \sigma_r(\sinh \alpha_r x - \sin \alpha_r x)] \quad (4)$$

where

$$\sigma_r = \frac{\sinh \alpha_r L_b - \sin \alpha_r L_b}{\cosh \alpha_r L_b + \cos \alpha_r L_b}$$

The orthonormality relations of mode shapes can be derived as follows [11]:

$$\int_0^{L_b} E_b I_b \phi_s(x) \frac{d^4 \phi_r(x)}{dx^4} dx = \begin{cases} \omega_r^2, & s = r \\ 0, & s \neq r \end{cases} \quad (5)$$

$$\int_0^{L_b} C_b \phi_s(x) \phi_r(x) dx = \begin{cases} 2\xi_r \omega_r, & s = r \\ 0, & s \neq r \end{cases} \quad (6)$$

$$\int_0^{L_b} \rho_b A_b \phi_s(x) \phi_r(x) dx = \begin{cases} 1, & s = r \\ 0, & s \neq r \end{cases} \quad (7)$$

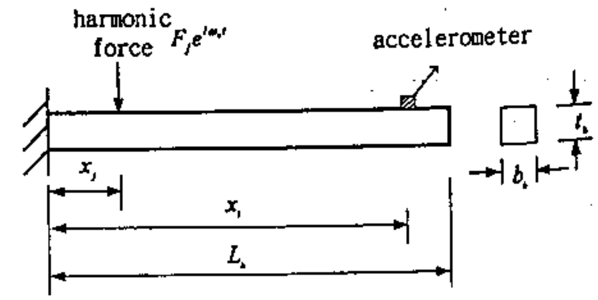

Fig. 1. Cantilever beam model

2.2 Harmonic analysis

For the beam subject to the harmonic force acting at $x = x_j$, the force function can be written:

$$F(x,t) = F_j \delta(x - x_j) e^{i\omega_s t} \tag{8}$$

The beam response can also be harmonic and determined

$$w(x,t) = \sum_{r=1}^{\infty} \phi_r(x) Q_r e^{i\omega_s t} \tag{9}$$

where

$$Q_r = \frac{F_j \phi_r(x_j)}{(\omega_r^2 - \omega_s^2) + i(2\xi_r \omega_r \omega_s)} \tag{10}$$

The beam response at $x = x_i$ can then be derived

$$w(x_i,t) = \sum_{r=1}^{\infty} \phi_r(x_i) Q_r e^{i\omega_s t} = e^{i\omega_s t} \sum_{r=1}^{\infty} \frac{F_j \phi_r(x_j) \phi_r(x_i)}{(\omega_r^2 - \omega_s^2) + i(2\xi_r \omega_r \omega_s)}$$

$$= X_i(\omega_s) e^{i\omega_s t} \tag{11}$$

where $X_i(\omega_s)$ is the harmonic response of the beam at $x = x_i$. If there are m observation points, the ODS vector can be defined as follows:

$$\{X(\omega_s)\} = \begin{Bmatrix} X_1(\omega_s) \\ X_2(\omega_s) \\ \vdots \\ X_m(\omega_s) \end{Bmatrix} = \begin{Bmatrix} |X_1(\omega_s)| e^{i\phi_1(\omega_s)} \\ |X_2(\omega_s)| e^{i\phi_2(\omega_s)} \\ \vdots \\ |X_m(\omega_s)| e^{i\phi_m(\omega_s)} \end{Bmatrix} \tag{12}$$

The frequency response function (FRF) between the j-th harmonic force and the i-th displacent response can also be obtained:

$$H_{ij}(\omega) = \frac{X_i}{F_j} = \sum_{r=1}^{\infty} \frac{\phi_r(x_j) \phi_r(x_i)}{(\omega_r^2 - \omega_s^2) + (2\xi_r \omega_r \omega_s)} \tag{13}$$

The input and output relation can be expressed as follows:

$$\{X(\omega)\} = [H(\omega)]\{F(\omega)\} \tag{14}$$

In conventional structural modal testing, one will experimentally measure a column or a row of the FRF matrix. Based on the theoretical formulation of FRF such as shown in Equation (13), modal parameter extraction method can then be applied to curve fit the FRF so that natural frequencies, damping ratios and mode shapes can be obtained.

In this work the ODS as defined in Equation (12) are assumed measurable. The harmonic force information is also assumed known in prior. Natural frequencies and damping ratios can be easily obtained from single measurement of FRF. The i-th components of ODS vector can be shown as a function of the harmonic force amplitude and the excitation frequency as well as modal parameters. The following section will present the mode shapes prediction model from the ODS.

2.3 Mode shape prediction model from ODS

The general idea for mode shape prediction from the measured ODS is illustrated in Fig. 2. There are m grid points in beam. With the assumption that the harmonic point force is applied at the j-th location, and the sensor, such as the accelerometer, is located at position i. The ODS vector $\{\hat{X}(\omega_s)\}_{m\times 1}$ can be measured and as the input data to the prediction model. As mentioned previously, natural frequencies and damping ratios of the beam structure can be easily obtained and also be the input. Through the prediction model, the structural mode shapes can then be determined. In order to develop the mode shape prediction model, the polynomial fit of the mode shape function is first illustrated in Fig. 3(a).

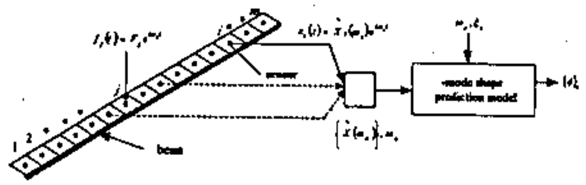

Fig. 2. Idea for mode shape prediction via ODS

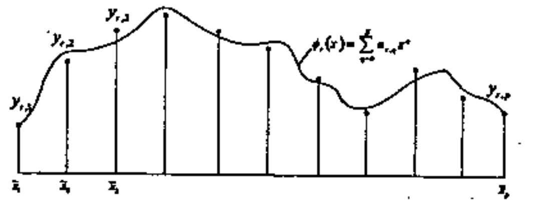

(a)Illustration for polynomial fit of mode shape function

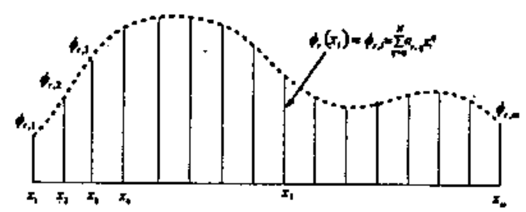

(b)Representation of mode shape by polynomial function

Fig. 3. Polynomial interpolation of mode shape function

There are p grid points along the beam length. Their coordinates are denoted as $\tilde{x}_1, \tilde{x}_2, \ldots, \tilde{x}_p$. Their corresponding components of the r-th mode shape are designated as $y_{r,1}, y_{r,2}, \ldots, y_{r,p}$. The polynomial fitting function for the r-th mode shape can be expressed as follows:

$$\phi_r(x)=\sum_{q=0}^{N} a_{r,q}x^q \qquad (15)$$

The coefficient $a_{r,q}$ can be determined by polynomial fit with the known x_s and. If there are m measurement points, and their coordinates are $x_1, x_2, \ldots, x_m$, then the i-th component of the r-th mode shape can be interpreted as illustrated in Fig. 3(b). There are several advantages of the adoption of polynomial fitting function to represent the mode shape. The number of interpolation point p can be different from the ODS measure point m. The order of polynomial function N can be easily adjusted for different boundary characteristics. In the following derivation of the mode shape prediction model, the will be chosen as the design variables. The slight deviation of from the mode shape components $\phi_r(\bar{x}_i)$ will still be smoothed. The polynomial fitting function still has good interpolation of structural mode shapes.

The purpose of this section is to formulate the optimization problem that can be solved for the mode shapes from ODS. As noted previously, the measured ODS vector is denoted $\{\hat{X}(\omega_i)\}$. The theoretical ODS vector $\{X(\omega_i)\}$ has been derived in section 2.2. As shown, $\{X(\omega_i)\}$ are functions of the harmonic force as well as modal parameters. In particular, the mode shape components are unknown and to be determined. Therefore, the optimization problem to predict the mode shape is defined as follows:

Objection function:

$$\Phi=\Phi(y_{r,s})=\left[MAC\left(\{X(\omega_i)\},\{\hat{X}(\omega_i)\}\right)-1\right]^2 \qquad (16)$$

Design variables:

$y_{r,s}; r=1,2,\ldots,n; s=1,2,\ldots,p$

Constraints:

I. $\begin{cases} MAC(\{\phi\}_r,\{\phi\}_s)-1\le 0, r=s \\ MAC(\{\phi\}_r,\{\phi\}_s)\le 0, r\ne s \end{cases}$

II. $S_r=\sum_{i=1}^{m}|\phi_{r,i}|, S_1>S_2>S_3>\ldots>S_n$

III. $S_{dr}=\sum_{i=1}^{m}|(\phi'_{r,i})|, S_{d1}<S_{d2}<S_{d3}<\ldots<S_{dn}$

The objective function uses the MAC characteristics. If two vectors are proportional to each other, the MAC value will be exactly one. The objection function is based on the least square error between the predicted and measured ODS. As shown in Equation (11), the predicted ODS $\{X(\omega_i)\}$ can be a function of the harmonic force and modal parameters. With the adoption of polynomial fit on mode shape functions as shown in Equation (15). The design variables can be specified as $y_{r,s}$. This approach is different from the previous work [8,9]. They used mode shape components as the design variables for MDOF systems. The polynomial fit will reduce the number of design variables and provide with flexibility to choose the interpolation points.

Constraint I is to confine the determined mode shapes to maintain their orthorgonality relations. Constraint II uses the sum of absolute value of mode shape components for each mode shape to adjust the mode sequence. Constraint III is also applied to adjust the mode sequence by summing the absolute values of derivative of mode shape components. The higher mode results in higher values of S_{dr}.

After the resolution of the optimization problem, design variables $y_{r,s}$ can be determined. The polynomial fit of mode shape function as shown in Equation (15) can also be solved. The mode shapes can then be interpolated accordingly.

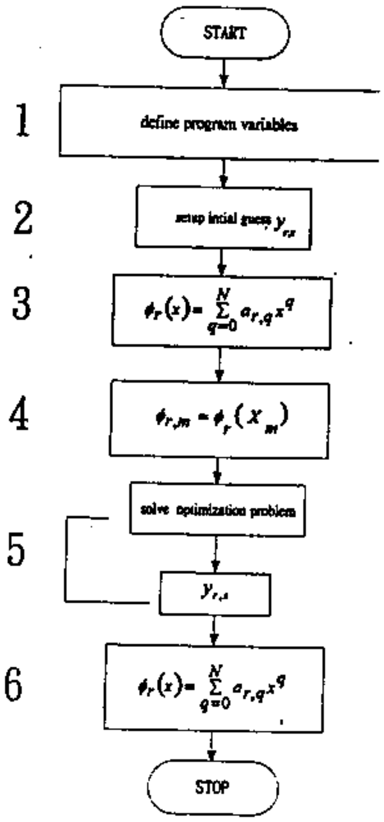

Fig. 4. Mode shape prediction program flow chart

3. Development of prediction program

This section introduces the mode shape prediction program by using MATLAB [12]. Polynomial-fit algorithm polyfit provided by MATLAB is adopted to curve fit the mode shape function with the known $\bar{x}_s$ and $y_{r,s}$, $s = 1,2,\ldots,p$. In solving the defined optimization problem, a general constrained optimization solver const also provided MATLAB is used. The solution flow chart is illustrated in Fig. 4.

The factors that affect the optimum solution and the accuracy of the predicted mode shapes are discussed as follows:

1. The number of interpolation points p should be proper selected. p must be large enough to reveal the mode shape characteristics. The thumb rule is that p is at least twice of modes to be predicted.
2. The order of polynomial function N should also be selected according to the number of modes to be determined.
3. The proper choice of the initial guess of design variables $y_{r,s}$ will be beneficial to efficiently solve for the optimum. As discussed, this work adopts the polynomial function to fit mode shapes. Therefore, the discrepancy of the guessed initial design variables from the optimum values can be adjusted accordingly. The fitted polynomials also have the ability to smooth the mode shape curve, and so forth the relative deviation of $y_{r,s}$ can be smoothed. The effect of the prediction error of $y_{r,s}$ on mode shapes will also be reduced.

4. Experimental verification

This section presents the experimental analysis for measuring the ODS of the cantilever beam subjected to a harmonic force excitation. The measured ODS can then be used to predict the first four mode shapes of the beam. The experimental setup is shown in Fig. 5(a). BK3550, a dual channel analyzer, is used. The signal generator produces a harmonic signal connected to power amplifier (BK2706) as the input signal to induce shaker (BK4809) located at position $j=2$ as shown in Fig. 5(b). The impedance head (PCB288D01) adhered to the beam to measure the actual applied force and the driving point acceleration. The driving point response is designated as the reference point. An additional accelerometer (PCB309A) is applied as the roving sensor in order to measure the ODS of the beam.

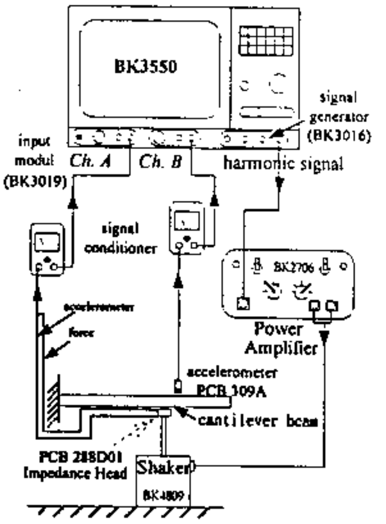

(a) Equipment setup

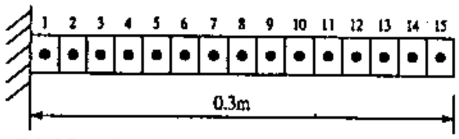

(b) Numbering of measurement point

Fig. 5. Experimental setup for measurement ODS

Table 1. Cantilever beam geometry dimension and material properties

Material	Steel
Length (L_b)	0.3m
Width (b_b)	0.0394m
Thickness (t_b)	0.0016m
Density (ρ_b)	7870kg/m^3
Young's Modulus (E_b)	207×10^9N/m^2

Table 2. Experimental measured natural frequencies and damping ratios

	Natural frequency (Hz)	Damping ratio
Mode 1	14.01	1.3478
Mode 2	90.73	1.123
Mode 3	253.45	0.455
Mode 4	488	0.3957

5. Experimental prediction of mode shapes

This section presents the experimental prediction of mode shapes from ODS to validate the developed prediction method. The beam geometry dimension and material properties in Table 1. The beam natural frequencies and damping ratios are first extract from single measurement of FRF by SDOF curve-fitting and tabulated in Table 2. The prediction program variables are set as the same as previous cases.

On-resonance excitation case

For the case of f_s=90Hz$\approx f_2$, i.e. near the second mode, Table 3 and Figure 6 show the experimental prediction results.

1.Table 3(a) shows the measured and predicted ODS as well as the relative errors for both time and frequency domain methods. The predicted ODS are generally about 3 times higher than the experimentally measured for the resonance excitation. The reason for the large discrepancy of amplitude could be the damping effect. However, the ODS as shown in Fig. 6(a) and 6(b) are still comparable and consistence.
2.Fig. 6(c) and 6(d) show the predicted mode shapes for both time and frequency domain ODS measurement methods, respectively. The predicted mode shapes generally agree very well. By examining the prediction error as shown in Table 3(b), one can observe that the error is generally with in 10% except at $i=1$ near the clamped end for its low amplitude.
3.From Table 3(c) and 3(d), the diagonal terms of MSF value are ranged from 1.03~1.12. This indicates the predicted mode shape errors are about 3%~12%. That the off-diagonal terms is almost close to zero indicates the well orthonormality relations.

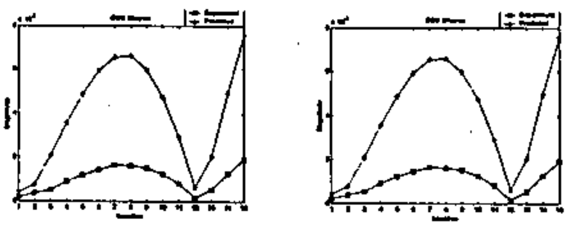

(a)ODS comparison for time domain method **(b) ODS comparison for frequency domain**

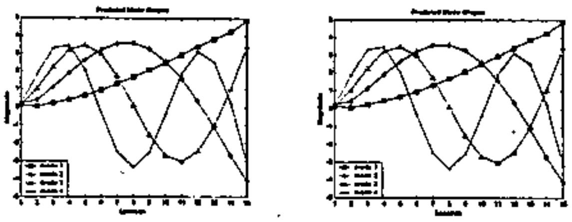

(c) Predicted mode shapes for time domain method **(d) Predicted mode shapes for frequency domain method**

Fig. 6. Experimental prediction of mode shapes for on-resonance excitation, f_s=90Hz$\approx f_2$

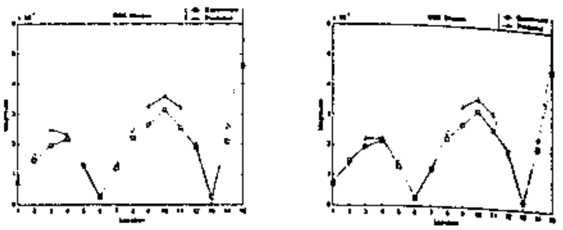

(a)ODS comparison for time domain method **(b) ODS comparison for frequency domain**

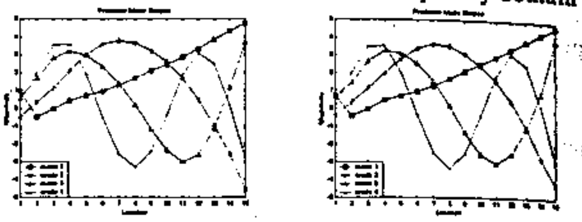

(c) Predicted mode shapes for time domain method **(d) Predicted mode shapes for frequency domain method**

Fig. 7. Experimental prediction of mode shapes for off-resonance excitation, $f_2 < f_s$=176Hz$< f_3$

Off-resonance excitation case

For the case of $f_2 < f_s$=176Hz $< f_3$, i.e. between the second and third modes, Table 4 and Figure 7 show the prediction results.

1.From Table 4(a) and Fig. 7(a) and 7(b), theODS prediction can be seen reasonably well.
2.The predicted mode shapes as shown in Fig. 7(c) and 7(d) reveal very good agreement except those near the clamped ends and nodal points.
3.The overall errors of mode shape prediction are ranged from –3% to 10% as observed from Table 4(c) and 4(d).

From above discussions, the developed mode shape prediction model is promising. For either on- or off-resonance excitation cases, the mode shape prediction can be satisfactory. Large discrepancy mainly occurs at those near the clamped and free ends or nodal points. This may due to the fact that the polynomial fit can not fit well for the boundary, especially for the fixed end. A refined spline-fit method may improve the improper interpolation at those critical areas. Besides, a good quality of ODS measurement is also desired in order to obtain the satisfactory prediction of mode shapes.

6. Conclusions

This work presents the mode shape prediction model from ODS. The structural ODS is defined as the steady state response of the structure subject to a harmonic force. The cantilever beam structure is studied and shown for the feasibility of the developed prediction model numerically and experimentally. The beam ODS response analysis is presented. The polynomial fit technique is also adopted to interpolate the mode shape function. Formulating the optimization problem then develops the mode shape prediction model. The main idea is to find the mode shapes such that the error between the measured and predicted ODS will be minimized.

Table 3. Experimental prediction of mode shapes for on-resonance excitation, f_s =90Hz ≈ f_2

(a) Comparison between theoretical and predicted ODS

	Time domain method			Frequency domain method		
	Measured	Predicted	Error (%)	Measured	Predicted	Error (%)
NO.	$\hat{X}\times10^{-4}$	$X\times10^{-4}$	$\frac{\lvert x\rvert-\lvert\hat{x}\rvert}{\lvert\hat{x}\rvert}\times100$	$\hat{X}\times10^{-4}$	$X\times10^{-4}$	$\frac{\lvert x\rvert-\lvert\hat{x}\rvert}{\lvert\hat{x}\rvert}\times100$
1	0.0124-0.0151i	0.0117-0.0395i	110.3627	-0.0155-0.0129i	0.0118-0.0399i	106.5930
2	0.0214-0.0305i	0.0227-0.0710i	100.1108	-0.0309-0.0209i	0.0234-0.0732i	105.9729
3	0.0284-0.0442i	0.0621-0.1995i	297.8018	-0.0450-0.0280i	0.0620-0.1991i	293.1071
4	0.0487-0.0785i	0.1042-0.3406i	285.5872	-0.0789-0.0478i	0.1040-0.3399i	285.4686
5	0.0617-0.1036i	0.1408-0.4679i	305.2500	-0.1049-0.0620i	0.1408-0.4679i	301.0091
6	0.0723-0.1241i	0.1683-0.5688i	313.0684	-0.1249-0.0727i	0.1683-0.5687i	310.3475
7	0.0639-0.1508i	0.1831-0.6293i	300.1775	-0.1409-0.0823i	0.1828-0.6283i	300.9543
8	0.0849-0.1386i	0.1820-0.6349i	306.4898	-0.1407-0.0819i	0.1815-0.6332i	304.5167
9	0.0781-0.1309i	0.1631-0.5767i	293.2867	-0.1314-0.0768i	0.1627-0.5755i	292.9087
10	0.0629-0.1065i	0.1269-0.4556i	282.4003	-0.1069-0.0622i	0.1270-0.4559i	282.6460
11	0.0413-0.0712i	0.0761-0.2803i	253.0394	-0.0711-0.0415i	0.0764-0.2817i	254.5342
12	0.0061-0.0158i	0.0132-0.0616i	272.1568	-0.0148-0.0071i	0.0133-0.0621i	287.2956
13	-0.0276+0.0450i	-0.0600+0.193i	284.1628	0.0454+0.0282i	-0.0606+0.195i	283.2865
14	-0.0670+0.1064i	-0.1406+0.4746i	293.6550	0.1077+0.0652i	-0.1414+0.477i	295.4172
15	-0.1018+0.1621i	-0.2137+0.7288i	296.6605	0.1647+0.0989i	-0.2129+0.7262i	293.9593

(b)Comparison between theoretical and predicted mode shapes

NO.	Time domain error (%) $([\hat{\phi}]-[\phi])/[\phi]\times100$				Frequency domain error (%) $([\hat{\phi}]-[\phi])/[\phi]\times100$			
	Mode 1	Mode 2	Mode 3	Mode 4	Mode 1	Mode 2	Mode 3	Mode 4
1	793.00	271.38	-15.17	-28.07	1162.00	275.54	3.39	-36.70
2	-39.89	-16.41	-10.90	-7.65	-56.90	-13.70	-11.90	-7.09
3	-2.52	-3.31	-11.01	-7.95	-2.35	-3.39	-11.00	-7.98
4	-2.26	-1.94	-10.99	-7.81	-0.45	-2.05	-10.85	-7.93
5	-5.10	-2.99	-11.02	-8.05	-4.72	-2.90	-11.01	-8.08
6	-5.29	-3.47	-11.06	-6.65	-5.66	-3.39	-11.16	-6.71
7	-4.49	-3.25	-11.04	-8.16	-4.78	-3.32	-11.16	-8.06
8	-4.22	-2.92	-9.50	-8.21	-4.19	-3.10	-9.01	-8.08
9	-4.52	-2.91	-11.10	-7.92	-4.31	-3.03	-11.16	-7.88
10	-4.61	-3.24	-10.99	-6.80	-4.45	-3.10	-10.98	-7.83
11	-4.07	-3.46	-11.02	-7.59	-4.01	-2.91	-10.98	-7.31
12	-3.46	-2.30	-11.17	-7.63	-3.42	-1.43	-11.18	-7.59
13	-3.95	-2.31	-11.00	-7.99	-3.86	-1.26	-11.00	-8.00
14	-5.25	-1.10	-12.57	4.04	-5.18	-0.47	-13.08	7.34
15	-0.99	-5.37	-9.69	-3.84	-1.06	-5.62	-9.34	-3.23

(c) MSF matrix for theoretical and predicted mode shapes (time domain method frequency)

theoretical predicted	Mode 1	Mode 2	Mode 3	Mode 4
Mode 1	**1.0364**	0.0070	-0.0054	0.0046
Mode 2	-0.0025	**1.0345**	0.0085	-0.0063
Mode 3	-0.0023	0.0133	**1.1218**	0.0092
Mode 4	0.0054	-0.0163	0.0138	**1.0806**

(d) MSF matrix for theoretical and predicted mode shapes (frequency domain method)

theoretical predicted	Mode 1	Mode 2	Mode 3	Mode 4
Mode 1	**1.0359**	0.0065	-0.0050	0.0041
Mode 2	-0.0022	**1.0344**	0.0079	-0.0058
Mode 3	-0.0027	0.0133	**1.1212**	0.0078
Mode 4	0.0059	-0.0161	0.0133	**1.0792**

Table 4. Experimental prediction of mode shapes for off-resonance excitation, $f_2 < f_s$ =176Hz $< f_3$

(a) Comparison between theoretical and predicted ODS

	Time domain method			Frequency domain method		
	Measured	Predicted	Error (%)	Measured	Predicted	Error (%)
NO.	$\hat{X}\times10^{-5}$	$X\times10^{-5}$	$\frac{\lvert x\rvert-\lvert\hat{x}\rvert}{\lvert\hat{x}\rvert}\times100$	$\hat{X}\times10^{-5}$	$X\times10^{-5}$	$\frac{\lvert x\rvert-\lvert\hat{x}\rvert}{\lvert\hat{x}\rvert}\times100$
1	0.0630-0.0336i	0.0865-0.0050i	0.0001	-0.0322-0.0640i	0.0800-0.0059i	0.0001
2	0.1212-0.0799i	0.1603-0.0173i	11.0734	-0.0803-0.1237i	0.1364-0.0146i	-7.0200
3	0.1666-0.1058i	0.2474-0.0298i	26.2867	-0.1081-0.1597i	0.2207-0.0271i	15.2776
4	0.1787-0.1210i	0.2292-0.0348i	7.4115	-0.1199-0.1778i	0.2200-0.0333i	3.7524
5	0.0838-0.0940i	0.1279-0.0331i	4.9007	-0.0741-0.1074i	0.1384-0.0331i	9.0958
6	-0.0224+0.0113i	-0.0055-0.0271i	110.2183	0.0111+0.0211i	0.0125-0.0278i	127.8481
7	-0.1009+0.0685i	-0.1355-0.0177i	12.0382	0.0676+0.1022i	-0.1240-0.0180i	2.2545
8	-0.1832+0.1257i	-0.2454-0.0052i	10.4544	0.1266+0.1856i	-0.2460-0.0047i	9.5284
9	-0.2183+0.1526i	-0.3249+0.0089i	22.0288	0.1558+0.2233i	-0.3321+0.0102i	22.0224
10	-0.2577+0.1802i	-0.3578+0.0218i	13.9983	0.1828+0.2640i	-0.3605+0.0226i	12.5172
11	-0.2091+0.1461i	-0.3214+0.0290i	26.5181	0.1486+0.2131i	-0.3128+0.0280i	20.8825
12	-0.1558+0.1104i	-0.1983+0.0263i	4.7947	0.1078+0.1599i	-0.1837+0.0239i	-3.9428
13	0.0241-0.0159i	0.0063+0.0123i	47.8641	-0.0152-0.0253i	0.0099+0.0114i	51.1561
14	0.1777-0.1092i	0.2606-0.0095i	25.0187	-0.1115-0.1751i	0.2398-0.0065i	15.5261
15	0.3897-0.2497i	0.5444-0.0330i	17.8196	-0.2538-0.3938i	0.5227-0.0344i	11.8014

Table 4. Experimental prediction of mode shapes for off-resonance excitation, $f_2 < f_s = 176\text{Hz} < f_3$

(b) Comparison between theoretical and predicted mode shapes

NO.	Time domain error (%) $([\hat{\phi}]-[\phi])/[\phi]\times 100$				Frequency domain error (%) $([\tilde{\phi}]-[\phi])/[\phi]\times 100$			
	Mode 1	Mode 2	Mode 3	Mode 4	Mode 1	Mode 2	Mode 3	Mode 4
1	9371.00	-911.81	225.46	85.57	7230.00	-743.26	299.45	-38.11
2	-650.34	-27.36	40.03	-2.18	-577.47	-21.78	23.18	1.61
3	-124.12	-4.07	10.61	-1.10	-102.91	-3.67	5.14	-3.02
4	-2.66	6.15	-10.91	-5.40	2.57	0.90	-10.22	-6.40
5	1.23	9.70	-24.28	-14.15	3.41	2.81	-20.07	-10.01
6	-5.73	7.71	-30.02	52.05	-5.16	1.99	-23.84	10.72
7	-5.98	3.02	-28.01	-5.03	-6.47	-0.98	-21.64	-7.49
8	-3.93	-1.53	98.04	-9.86	-4.15	-4.83	60.92	-8.80
9	-3.94	-3.88	-32.70	-11.76	-2.69	-7.92	-22.37	-8.93
10	-5.89	-2.93	-21.17	-16.99	-3.11	-8.35	-14.94	-9.16
11	-7.11	2.56	-11.80	-8.77	-3.97	-3.30	-10.35	-7.55
12	-5.82	39.46	-4.16	-8.38	-3.88	34.05	-7.96	-7.44
13	-3.39	-16.16	0.84	-9.16	-3.30	-12.32	-2.93	-8.42
14	-3.20	-5.77	-1.44	-40.67	-3.97	0.92	-21.42	-16.09
15	-3.90	4.78	-4.17	-16.61	-4.31	-3.66	3.74	-10.99

(c) MSF matrix for theoretical and predicted mode shapes (time domain method frequency)

theoretical / predicted	Mode 1	Mode 2	Mode 3	Mode 4
Mode 1	**1.0325**	0.0146	0.0078	0.0212
Mode 2	-0.0064	**0.9784**	-0.0235	-0.0258
Mode 3	-0.0124	0.0214	**1.1268**	0.0226
Mode 4	-0.0119	0.0123	0.0151	**1.0839**

(d) MSF matrix for theoretical and predicted mode shapes (frequency domain method)

theoretical / predicted	Mode 1	Mode 2	Mode 3	Mode 4
Mode 1	**1.0316**	0.1056	0.0116	0.0161
Mode 2	0.0021	**1.0245**	-0.0299	-0.0139
Mode 3	-0.0186	0.0267	**1.1023**	0.0232
Mode 4	-0.0035	0.0028	0.0046	**1.0772**

Both the numerical simulation and experimental verification are performed and validated, respectively, for the feasibility in determining mode shapes from ODS. This work will improve the restriction of conventional modal testing that requires the tested structure in static. In particular, for harmonic excitation system, such as a rotor system, the developed methodology can be applied. This work thus enhances the experimental modal analysis technique for the structure in harmonic operating condition.

7. Acknowledgement

The authors greatly thank the financial support of National Science Council under the Grant NO: NSC90-2212-E-020-004.

8. Reference

1. Ewins, D. J., 1986, *Modal Testing: Theory and Practice*, Research Studies Press LTD., Letchworth Hertfordshire, England.
2. James III, G. H., T. G. Carne and J. P. Laufer, 1995, "The Natural Excitation technique (NexT) for Modal Parameter Extraction from Operating Structures," *Journal of Analytical and Experimental Modal Analysis*, Vol. 10, pp. 260-277.
3. Hermans, L., and H. V. Auweraer, 1999, "Modal Testing and Analysis of Structures Under Operational Conditions : Industrial Applications," *Journal of Mechanical Systems and Signal Processing*, pp.193-216.
4. Hermans, V., and Hermans, L., 1999, "Applications of Structural Model Identification During Normal Operating Conditions: An Overview of the Eureka Project Sinopsys," *Proceeding of the 17th International Modal Analysis Conference*, Vol. 1, pp.27-34.
5. Marscher, W. D., and C. W. Jen, 1999, "Use of Operating Deflection and Mode Shapes for Machinery Diagnostics," *Proceedings of the 17th International Modal Analysis Conference*, Vol. 2, pp. 2065-2071.
6. Pascual, R., Folinval, J., C., and Razeto, M., 1999, "On Line Damage Assessment Using Operating Deflection Shapes," *Proceeding of the 17th International Modal Analysis Conference*, Vol. 1, pp.238-243.
7. Verhoeven, J., 1988, "Excitation Force Identification of Rotating Machines Using Operational Rotor/Stator Amplitude Data and Analytical Synthesized Transfer Functions," *Journal of Vibration, Acoustics, Stress, and Reliability in Design*, pp. 307-314.
8. Wang, B. T., 2001, "Determination of Mode Shapes from the Operational Deflection Shape," The 8th International Congress on Sound and Vibration, pp. 1941-1948.
9. Hu. H. L., 2001, *Modal Analysis of Structures System under Operational Condition*, Master Thesis, Department of Mechanical Engineering National Pingtung University of Science and Technology.
10. Belvins, R. D., 1995, Formulas for natural frequencies and mode shape, Krieger Publishing Company, Malabar, Florida, pp.108.
11. Wang, B. T., 1998, "Structural Modal Testing with Various Actuators and Sensor," *Journal of Mechanical Systems and Signal Processing*, pp.627-639.
12. MATHWORK Inc., 1997, MATLAB User Manual.